RESEARCH ARTICLE

A Comprehensive Study on the Mechanical Properties of Bulldozing Plate Soil Engaging Surface Based on the Entropy-Weighted Grey Relational Analysis Method

ZHIJUN GUO[ID]**1, (Member, IEEE), SHUAI ZHANG**[ID] **1, (Member, IEEE), AND LIWEI NI**[2]
[1]College of Vehicle and Traffic Engineering, Henan University of Science and Technology, Luoyang 471003, China
[2]College of Mechanical Engineering, Henan University of Engineering, Zhengzhou 451191, China

Corresponding author: Shuai Zhang (boreke@126.com)

ABSTRACT To reduce the working resistance and soil adhesion in the process of soil tillage or engineering construction, this paper takes the bulldozing plate as the research object and takes the cutting angle and the directrix form of the Soil engaging surface as the design variables and designs 15 groups of bulldozing plate models for the soil bin experiments. The test results show that compared with the conventional circular bulldozing plate, the horizontal working resistance of the bionic bulldozing plate with 50 degrees, 55 degrees, and 60 degrees cutting angles is reduced by 44.46 %, 39.74 %, and 10.32 %, respectively. 55 degrees cutting angle bionic bulldozing plate to reduce adhesion and front soil fluctuations best; each performance index of the parabolic bulldozing plate is relatively balanced and stable. An entropy-weighted grey relational analysis method is proposed to quantitatively analyze and sort the comprehensive performance of bulldozing plates. Then, the influence law between the horizontal resistance, vertical resistance, and the total resistance of the bulldozer during stable operation and soil adhesion and soil fluctuation state is studied. The hypothesis of the internal influence relationship between the intrinsic micro-geometric characteristics and the macroscopic comprehensive mechanical properties of the soil engaging surface of the bulldozing plate is proposed, and it is pointed out that the essence of the change of the cutting angle and the directrix form of the soil engaging part is the change of the directrix curvature of the soil engaging surface and the soil. It is proposed to optimize and edit the directrix curvature trend of the soil engaging surface and then reverse the directrix equation so as to realize the optimal design of the soil engaging surface. The research in this paper provides a reference for the design and optimization of reducing adhesion and resistance of soil engaging components.

INDEX TERMS Bulldozing plate, soil engaging surface, bionics, entropy-weighted grey relational analysis, reducing adhesion and resistance.

I. INTRODUCTION

Humans consume a lot of energy daily to complete agricultural soil tillage and various engineering construction operations, and even gradually expand to seabed exploration and planetary development. The relevant soil engaging components or soil-cutting tools consume about 40-60% of the

The associate editor coordinating the review of this manuscript and approving it for publication was Jiajia Jiang[ID].

power of the whole machine during the working process, trying to reduce its working resistance, is of great significance to energy conservation and emission reduction.

In the process of long-term soil environment life, some animals in nature have evolved their claws and toes for hundreds of millions of years and gradually formed excellent biomechanical functions. Its specific curved claw toe shape not only reduces adhesion between the claw toe and the soil during excavation but also has extremely low working
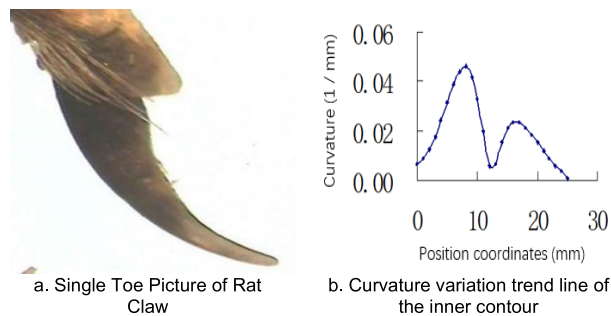
a. Single Toe Picture of Rat Claw

b. Curvature variation trend line of the inner contour

FIGURE 1. Inner-contour geometric line features of vole claw toe.

resistance. This provides a bionic research idea for the design of soil engaging surface geometry of various soil working components to reduce resistance.

To solve these problems cutting tools often suffer from low efficiency, poor quality, and high energy consumption due to adhesion, abrasion, or friction on the surface; several scholars have introduced bionics into the design of tools [1]. Yu et al. [2] designed a bionic potato digging shovel based on mole rat's digits using a biomimetic macroscopic surface modification method and verified its feasibility and effectiveness. Yang et al. [3] developed efficient tillage or digging tools inspired by the geometric structure of the mole's five claws to minimize the soil shear resistance of the optimal blade. The geometric characteristics of dozens of paws and toes of some animals (including mole crickets, roosters, house mice, ground squirrels, pangolins, ants, etc.) with excellent digging functions were analyzed. The results showed that the curvatures of the inner and outer contour lines of paws and toes, especially the curvature of the inner contour line, had fluctuating characteristics and were not the simple circular or parabolic surfaces imagined [4], [5], [6], [7]. So, does this bionic soil engaging surface with variable curvature have better resistance reduction characteristics than a simple circular arc surface or parabolic surface? If so, what kind of resistance reduction mechanism does it have? How does it achieve the adhesion and resistance reduction function?

Inspired by this, the exploration of the general form of ideal soil engaging surfaces in this paper was carried out, and the characteristic curves (bionic lines) of the inner contours of typical vole paw-toe soil engaging surfaces were extracted and studied based on the geometric analysis of various typical soil animal paw-toes in the early stage, as shown in Figure 1.

As the bulldozer's main working part, the bulldozer plate's power occupies about 40% of the effective power of the bulldozer engine in the working process [4]. The complex working environment often makes the bulldozing plate soil engaging surface to increase the working resistance and reduce the working efficiency due to the severe soil adhesion [8], [9]. Trying to reduce the adhesion of the soil to the soil engaging of the bulldozing plate and reduce the

working resistance of the bulldozing plate has become the main research objective.

Researchers have proposed various surface resistance reduction techniques for soil working components. Based on the imitation of an earthworm back-hole jet, Gu et al. [10] studied the drag reduction mechanism of the bionic jet surface. Pneumatic subsoiling not only improved the small stress problem of conventional subsoiling but also increased the disturbance of soil by gas based on conventional subsoiling, which achieves the effect of subsoiling and reducing resistance and consumption [11]. Zuo et al. [12] conducted a simulation experiment to observe the internal and external changes of the soil before and after air pressure subsoiling with 3 indices, including soil porosity, soil porosity increasing rate, and soil surface uplift. The results showed that for the effective radius of impact on the land surface, air pressure subsoiling was about 2-2.5 times higher than conventional subsoiling and at least 3 times higher on the plow pan. Zhang et al. [13] even tried to reduce the working resistance of soil working parts utilizing local explosive shocks, and the resistance reduction effect was up to 25% for a given operating condition. This high-pressure fluid injection lubrication method has played a good role in reducing resistance but also faces many ancillary devices, additional energy consumption, and high-cost disadvantages. Keppler et al. [14] found during discrete element modeling of soil-tool interactions that the free vibration of the tillage tool induced by soil-tool interaction had a significant effect on the measured draft force. Liu et al. [15] explored the vibration response characteristics of soil under sinusoidal vibration and the mechanism of soil detachment, indicating that reasonable setting of vibration parameters can improve the soil detachment performance of the adhesion system at the interface between soil and metal surfaces. Niyamapa and Salokhe [16] found that both the horizontal force and vertical force of the blade of the vibration tillage tools decreased with the increase in oscillating frequency. Although the vibration mode can reduce the working resistance, the vibration system makes the machine structure complex; the cost will be correspondingly increased and accompanied by the generation of parasitic power. The bionic electroosmosis method has a good effect on solving the adhesion problem of some soil engaging components, but it is limited when applied to high-speed tangential sliding soil working components such as bulldozing plates [17]. Massah et al. [18] designed a soil engaging plate with optimized operating parameters using biomimetic electro-permeation technology, which reduced the soil adhesion of the plate by 29.8% to 90% compared to conventional plates. The bionic non-smooth technology is used to reduce the working resistance of the soil engaging surface of the bulldozing plate. Through the selection of non-smooth convex pack forms such as spherical and corrugated, the distribution law and the optimization design of specific structural parameters, the contact state between the soil and the soil engaging surface of the bulldozing plate is changed. Then

the desorption effect of the soil relative to the soil engaging surface is improved, and the overall working resistance is reduced [19], [20]. Chirende et al. [21] applied the concept of bionic non-smooth surfaces to disc plows in their research to reduce soil resistance. The results from the indoor soil bin experiments showed that the convex bionic units had the highest resistance reduction of 19% compared to the concave bionic units. Wu et al. [22] obtained the non-smooth surface morphology of the antlion by scanning electron microscopy and established the motion model of the non-smooth surface in soil, and deduced that the height of the non-smooth drag-reducing surface bump is proportional to the square of the distance between two bumps and inversely proportional to the square of the motion velocity.

The above-mentioned fluid injection lubrication, vibration, bionic electro-osmosis, and bionic non-smoothing methods can achieve the purpose of desorption drag reduction to a certain extent. However, these methods are difficult to promote due to poor wear resistance, complex processing technology, excessive auxiliary parts, extra energy loss, and other issues. Reasonable optimization of the macroscopic geometry of the bulldozing plate can effectively reduce the adhesion and working resistance of the soil to the soil engaging surface. The resulting soil working components have the characteristics of simple structure, reliable operation, low maintenance cost, and low additional energy consumption.

Therefore, scholars have been exploring optimizing the shape of the bulldozing plate's macroscopic soil engaging surface and establishing a reasonable mathematical model of the soil engaging surface to reduce the adhesion and working resistance of the soil to the soil engaging surface. Niu et al. [23] investigated the effect of different bionic surfaces on tillage resistance by finite element simulation and experiment. The results indicated that the bionic tiller with discontinuous microstructures reduced the horizontal and vertical forces by 21.3% and 24.8%, respectively. Zhao et al. [24] studied the effect of different edge curve geometries on torque requirements and soil disturbance characteristics. As the sliding cutting angle of the edge curve tip increased, the average torque requirement decreased, and fewer soil particles were thrown upward. He et al. [25] developed blades with three lengths of horizontal plates and different cutting rake angles to perform soil cutting and bulldozing experiments. The results showed that the blade with horizontal plates could reduce the working resistance of the soil engaging surface when the rake angle was greater than a certain threshold. Li et al. [26] developed a numerical model using the discrete element method to simulate the interaction between the bear claw with soil, and the results showed that the draft and vertical force varied linearly and nonlinearly with the raking angle of the claw, respectively. It is not enough to reduce the working resistance of the soil engaging surface by changing the cutting angle. The blade shape affects the cutting resistance of the blade and can be designed to reduce the working resistance of the tillage implements. He et al. [27]

studied the effect of cutting depth and horizontal plate length on the cutting resistance of the blade through soil cutting experiments, and the results showed that when the cutting depth is the same, the cutting resistance firstly decreases and then rises with the increase of the horizontal plate length. Hoseinian et al. [28] developed a dual sideway-share subsurface tillage tool with a total cutting width of 53 cm and harrow and tilt angles of 15 and 10 degrees, respectively, using the discrete element method modeling to optimize its geometry. The concave cutting edges of the no-tillage opener can reduce soil disturbance relative to straight and convex cutting edges [29]. Gill and Vandenberg [30] pointed out early that the design of curved soil engaging surfaces can effectively reduce the working resistance of soil-working components. In engineering practice, the soil engaging surface of the bulldozing plate is mostly in the form of a circular arc or a combined circular arc-linear combination [30], [31], [32]. Parabolic plow surface is often used in agricultural soil tillage and has a good effect of adhesion and resistance reduction [33].

In addition to circular and parabolic surfaces, the author's previous studies have shown that certain contour curves of the paw-toe soil engaging surfaces of animals with excellent digging function, when used as the soil engaging surface directrix of deep loosening shovel by bionic design, can reduce the resistance up to 35% compared with the circular arc type deep loosening shovel, and the maximum resistance reduction up to 60% compared with the straight pattern surface deep loosening shovel [31], [34], [35].

Therefore, to optimize the macroscopic geometry of the macroscopic soil engaging surface of the bulldozing plate is mainly to optimize the directrix and the curvature of the directrix forming the soil engaging surface, thus affecting the normal pressure on the soil sliding across the soil engaging surface and the slip or slip crack surface of the soil being cut, and then affecting the total working resistance and soil fluctuation effect, to achieve the purpose of reducing adhesion and resistance. In this paper, a series of preferably selected bulldozing plates with different curvature directrix are tested. The influence law between the form of bulldozing plate's directrix and mechanical properties is explored by combining the entropy-weighted gray relational analysis method. The hypothesis is put forward to provide a reference for the design of bulldozing plates to reduce adhesion and resistance.

II. METHODOLOGY
A. CONTRIBUTION ANALYSIS METHOD
The contribution analysis method mainly uses the regression of DOEs to calculate the contribution, which is used for ranking the contribution of design variables to the performance target and screening the design variables in high dispersion or high nonlinearity analysis to reduce the computational cost and improve the efficiency of optimal design, and its analytical calculation steps are as follows.

Step 1: Normalize processing

A DOEs approach was used to obtain a sample of experiments between design variables and response characteristics. The design variables have different design spaces, contribution values also change in the design space, and the sample data input needs to be normalized using formula (1):

$$x_i^* = \frac{x_i - \bar{x}}{\sigma} = \left(x_i - \frac{1}{N} \sum_{i=1}^{N} x_i \right) \times \left[\sqrt{\frac{1}{N} \sum_{i=1}^{N} (x_i - \bar{x})^2} \right]^{-1} \quad (1)$$

where $\bar{x}$ is the average value of the sample data; σ is the standard deviation; N is the total number of sample data; x_i is the original input, and x_i^* is the normalized input.

Step 2: Contribution analysis

If there are k design variables $(x_1, x_2, \ldots, x_k)$, then any response characteristic can be expressed by a multiple regression model as:

$$P(x_1, x_2, \ldots, x_k) = \mu + \sum_{i=1}^{k} Q_i(x_i)$$
$$+ \ldots + \sum_{i=2}^{k} \sum_{j=1}^{k-1} R_{ij}(x_i, x_j) + \varepsilon \quad (2)$$

where $P(x_1, x_2, \ldots, x_k)$ is any response characteristic; $\sum_{i=1}^{k} Q_i(x_i)$ is the main effect of the design variable; $\sum_{i=2}^{k} \sum_{j=1}^{k-1} R_{ij}(x_i, x_j)$ is the crossover effect of any two design variables; μ is a constant term and ε is the deviation.

The main effect of the design variable can be expressed by formula (3):

$$\sum_{i=1}^{k} Q_i(x_i) = \sum_{i=1}^{k} \hat{\beta}_i x_i \quad (3)$$

Therefore, the contribution of the design variables can be defined by formula (4):

$$N_{x_i} = \frac{100\hat{\beta}_i}{\sum_i |\hat{\beta}_i|} i = 1, 2, \ldots, k \quad (4)$$

where $\hat{\beta}$ is calculated coefficient of design variable x_i using the least squares estimation method and N_{x_i} is the corresponding contribution of design variable x_i.

B. GREY RELATIONAL ANALYSIS

GRA is a method that uses grey relational grade (GRG) to measure the degree of approximation between the experimental and ideal sequences. It is widely used in multi-objective and multi-decision optimization problems and has comprehensive advantages in solving complex decision-making problems [26]. The specific steps of GRA are as follows:

Step 1: Data pre-processing

Due to the different orders of magnitude of experimental data, GRA may not be able to obtain reliable, optimal

solutions, so it is necessary to convert the experimental data into a set of dimensionless data between 0.00 and 1.00 for further quantitative analysis. Different data pre-processing techniques can be used according to the response characteristics.

If the response characteristic has the characteristics of "bigger is better," the normalization method can be expressed as:

$$x_i^*(k) = \frac{x_i(k) - min_k x_i(k)}{max_k x_i(k) - min_k x_i(k)}$$
$$(k = 1, 2, \cdots n; i = 1, 2, \cdots m) \quad (5)$$

If the response characteristic has the characteristic of "lower is better," the normalization method can be expressed as:

$$x_i^*(k) = \frac{max_k x_i(k) - x_i(k)}{max_k x_i(k) - min_k x_i(k)}$$
$$(k = 1, 2, \cdots n; i = 1, 2, \cdots m) \quad (6)$$

If the response characteristic is ideal concerning a specific value, the normalization method can be expressed as:

$$x_i^*(k) = 1 - \frac{|x_i(k) - T|}{max[max_k x_i(k) - T, T - min_k x_i(k)]}$$
$$(k = 1, 2, \cdots n; i = 1, 2, \cdots m) \quad (7)$$

where $x_i^*(k)$ is the k-th response characteristic value of the i-th experiment after normalization; $x_i(k)$ is the initial design value of response characteristic; $min_k x_i(k)$ and $max_k x_i(k)$ is the minimum and maximum value of all response characteristics $x_i(k)$, $k = 1, 2, \ldots, n$; $i = 1, 2, \ldots, m$; m is the number of experiments; n is the number of response characteristics, and T is the specific value.

Step 2: Calculate the grey relational coefficient (GRC)

The GRC of the k-th response characteristic of the i-th experiment is expressed as:

$$\gamma(x_0^*(k), x_i^*(k)) = \frac{\triangle_{min} + \zeta \triangle_{max}}{\triangle_{0i}(k) + \zeta \triangle_{max}} \quad (8)$$

where $x_0^*(k)$ is the experimental reference sequence; $x_i^*(k)$ is the initial experimental sequence; $\triangle_{0i}(k) = |x_0^*(k) - x_i^*(k)|$ is the absolute difference between $x_0^*(k)$ and $x_i^*(k)$; $\triangle_{max} = \max_i \max_k \triangle_{0i}(k)$ and $\triangle_{min} = \min_i \min_k \triangle_{0i}(k)$ are the maximum and minimum values of $\triangle_{0i}(k)$, respectively; ξ is the distinguishing coefficient, $\xi \in [0,1]$, which is generally defined as 0.5.

Step 3: Calculate the GRG

The GRG is calculated by averaging the GRC and expressed as:

$$\Gamma(x_0^*, x_i^*) = \frac{1}{n} \sum_{k=1}^{n} \gamma(x_0^*(k), x_i^*(k)) \quad (9)$$

where Γ is the GRG, and n is the number of response characteristic.

According to formula (9), the GRG of each design scheme can be obtained. According to the size of GRG, each design

scheme can be sorted to obtain the optimal scheme with comprehensive performance. The design scheme with the highest GRG value through calculation represents the scheme with the best comprehensive performance.

C. ENTROPY-WEIGHTED GREY RELATIONAL ANALYSIS (EGRA)

The entropy weight method is used to determine the weight of objective function. The higher entropy weight, the greater the weight of objective function in the optimization process.

The mapping function $f_i:[0,1] \rightarrow [0,1]$ applied in the entropy must satisfy the following three conditions, $f_i(0) = 0$, $f_i(x) = f_i(1)-x)$, and $f_i(x)$ must be monotonically increasing in interval $x \subset (0,0.5)$; Therefore, the function $w_e(x)$ is defined as the mapping function of the entropy weight method:

$$w_e(x) = xe^{(1-x)} + (1-x)e^x - 1 \qquad (10)$$

where $w_e(x)$ takes its maximum value at $x = 0.5$, $w_e(0.5)=0.6487$. At the same time, to ensure that the mapping function can take values within the range [0,1], the following new entropy is defined:

$$W = \frac{1}{(e^{0.5} - 1)n} \sum_{i=1}^{n} w_e(x_i) \qquad (11)$$

According to the above definition and the GRC, the steps for determining the weight of each objective function are as follows:

(1) In all design schemes, the sum of the GRC corresponding to the k-th response characteristic:

$$T_k = \sum_{i=1}^{m} \gamma\left(x_0^*(k), x_i^*(k)\right) (k = 1, 2, 3, \cdots \cdots n) \qquad (12)$$

(2) Normalize the coefficients:

$$N_c = \frac{1}{(e^{0.5} - 1)m} = \frac{1}{0.6487m} \qquad (13)$$

(3) The entropy of each response characteristic can be written as:

$$e_k = N_c \sum_{i=1}^{m} w_e\left(\frac{\gamma\left(x_0^*(k), x_i^*(k)\right)}{T_k}\right) (k = 1, 2, 3, \cdots \cdots n) \qquad (14)$$

(4) The sum entropy can be expressed as:

$$E = \sum_{k=1}^{n} e_k \qquad (15)$$

(5) The relative weight can be calculated as follows:

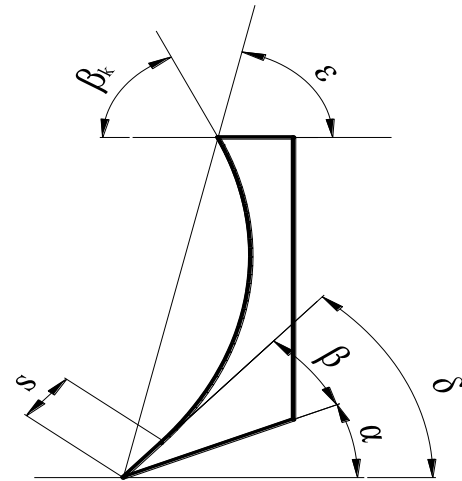$$\beta_k = \frac{1}{m - E}(1 - e_k) \qquad (16)$$

FIGURE 2. Diagram of the angle parameters of the bulldozing plate.

(6) The weight of the k-th response characteristics can be written as:

$$\omega_k = \frac{\beta_k}{\sum_{i=1}^{n} \beta_i} \qquad (17)$$

Since each response characteristic's relative significance may differ, the simple averaging method of formula (9) may lead to an inaccurate evaluation of the GRG. Therefore, according to formula (17), the weight of each response characteristic can be obtained, and different weights are assigned to the response characteristic to carry out EGRA:

$$\Gamma\left(x_0^*, x_i^*\right) = \sum_{k=1}^{n} \omega_k \gamma\left(x_0^*(k), x_i^*(k)\right) \qquad (18)$$

where ω_k is the weight of the k-th response characteristic.

According to formula (18), EGRA sorting can be performed to obtain optimal comprehensive performance solutions. The design with the highest EGRA value represents the best overall performance.

III. DESIGN AND MACHINING OF BULLDOZING PLATE STRUCTURE

A. BULLDOZING PLATE DESIGN PARAMETERS

The guiding effect of the soil-engaging surface on the soil is reflected in the cutting angle of the bulldozing plate, the rear angle α, the tip angle of the shovel β, the front flip angle β_k, and the oblique mounting angle ε, which should meet the requirements of actual production, good guiding restraint will improve the efficiency of the bulldozing plate and the performance of disengagement and drag reduction [36], Figure 2 shows the schematic design of the structure of the bulldozing plate, where the left line is the directrix of the soil-engaging surface of the bulldozing plate.

B. BULLDOZING PLATE DIRECTRIX FORMS

Based on the study of the soil-engaging surface of conventional bulldozing plates, the authors found, Different Directrix forms were designed by varying the trend of Directrix

TABLE 1. Directrix equations.

Cutting angle	Directrix forms	Directrix equations
50º	circular arc	$y = -(-x^2+155.300\,x+27730.870)^{0.5} + 166.520$
	Parabola	$x=0.405\,t+7.744\,t^{0.5}$ $y=0.332\,t-4.073\,t^{0.5}$
	Cycloid	$x=0.0000212716\ 6235\,t^3-0.0082836102\ 2249\,t^2+1.7862656127\ 47t$ $y=-0.0000266616\ t^3+0.0103825415\ 6t^2-0.9573747750\ 4t$
	Involute	$x=0.0000194347\ 07748\,t^3-0.0065562749\ 89734\,t^2+1.5685217209\ 23t$ $y=-0.0000295779\ t^3+0.0099780655\ 34t^2-0.8311499217\ t$
	Bionic Line	$x=0.007758047\ t^4-0.056892349\ t^3-0.1926581861\ t^2+10.037171287\ t$ $y=0.0070245124\ t^4-0.051513098\ t^3-0.17444205\ t^2-2.627550761\ t$
55º	circular arc	$y=-(-x^2+155.300\,x+45513.100)^{0.5}+213.340$
	Parabola	$x=0.405\,t+7.744\,t^{0.5}$ $y=0.26588\,t-3.25788\,t^{0.5}$
	Cycloid	$x=0.0000212716\ 62354\,t^3-0.0082836102\ 2419\,t^2+1.7862656167\ 47t$ $y=-0.0000211865\ t^3+0.0082504124\ 6t^2-0.7607710269\ 3t$
	Involute	$x=0.0000194347\ 078748\,t^3-0.0065562749\ 08734\,t^2+1.5685217429\ 23t$ $y=-0.0000240117\ 877\,t^3+0.0081003652\ 261t^2-0.6747742610\ 661t$
	Bionic Line	$x=0.0077580476\ t^4-0.0568923497\ t^3-0.1926581861\ t^2+10.0371714287\ t$ $y=0.0052553759\ t^4-0.0385394243\ t^3-0.1305085047\ t^2-1.9657967984\ t$
60º	circular arc	$y=-(-x^2+155.300\,x+83982.480)^{0.5}+289.790$
	Parabola	$x=0.405\,t+7.744\,t^{0.5}$ $y=0.205\,t-2.515\,t^{0.5}$
	Cycloid	$x=0.0000212716\ 62584\,t^3-0.0082836122\ 2419\,t^2+1.7862656167\ 47t$ $y=-0.0000164254\ 49t^3+0.0063963872\ 16t^2-0.5898112456\ 3t$
	Involute	$x=0.0000194347\ 07878\,t^3-0.0065562740\ 89734\,t^2+1.5685217420\ 23t$ $y=-0.0000183920\ 0799\,t^3+0.0062045350\ 66799\,t^2-0.5168241329\ 868t$
	Bionic Line	$x=0.0077580476\ t^4-0.056892497\ t^3-0.192658861\ t^2+10.037171287\ t$ $y=0.0039362765\ t^4-0.0288660288\ t^3-0.09775087\ t^2-1.47238802\ t$

curvature and applied to the design of the soil-engaging surface of the bulldozing plate, Achieving good results [34]. In this paper, we select circular, parabolic, cycloidal, involute, and bionic quasi-linear forms of bulldozing plate to study, The Directrix equations of each soil-engaging surface for cutting angles of 50°, 55°, and 60° are shown in Table 1, The directrix forms are shown in Figure 3.

C. BULLDOZING PLATE REDUCTION MODEL PROCESSING
Combined with the design parameters of the bulldozing plate in Figure 2 and Table 1, 15 test equal scale reduced bulldozing plates were designed, and the design parameters of each bulldozing plate are shown in Table 2. The height and degree

of the test bulldozing plate are 150mm and 300mm respectively, and the height-to-width ratio is 0.5. The completed test bulldozing plate is shown in Figure 4. The bulldozing plate is circular, parabolic, cycloidal, involute, bionic, and linear, from left to right, Each Directrix form has three bulldozing plates with cutting angles of 50°, 55°, and 60° in that order.

IV. BULLDOZING PLATE WORKING RESISTANCE ANALYSIS
A. BULLDOZING PLATE WORKING RESISTANCE TEST
1) TEST EQUIPMENT
The required equipment for the test is shown in Table 3, and the corresponding test equipment is shown in Figure 5.

TABLE 2. The specific parameters of bulldozing plate.

Bulldozing plate number	Structural parameters of soil-touching surfaces					
	Directrix form	Cutting angle δ	Front flip angle β_k	Oblique mounting angle ε	Rear angle α	The tip angle of the shovel β
1		50°	72.1°			
2	Circular arc	55°	75.4°			
3		60°	78.7°			
4		50°	68.7°			
5	Parabola	55°	72.2°			
6		60°	76.8°			
7		50°	67.5°			
8	Cycloid	55°	69.5°	75°	20°	30°
9		60°	71.5°			
10		50°	67.9°			
11	Involute	55°	72.5°			
12		60°	76.9°			
13		50°	65.8°			
14	Bionic Line	55°	68.6°			
15		60°	70.5°			

a. Circular arc   b. Parabola   c. Cycloid   d. Involute   e. Bionic Line   f. Directrix Collection
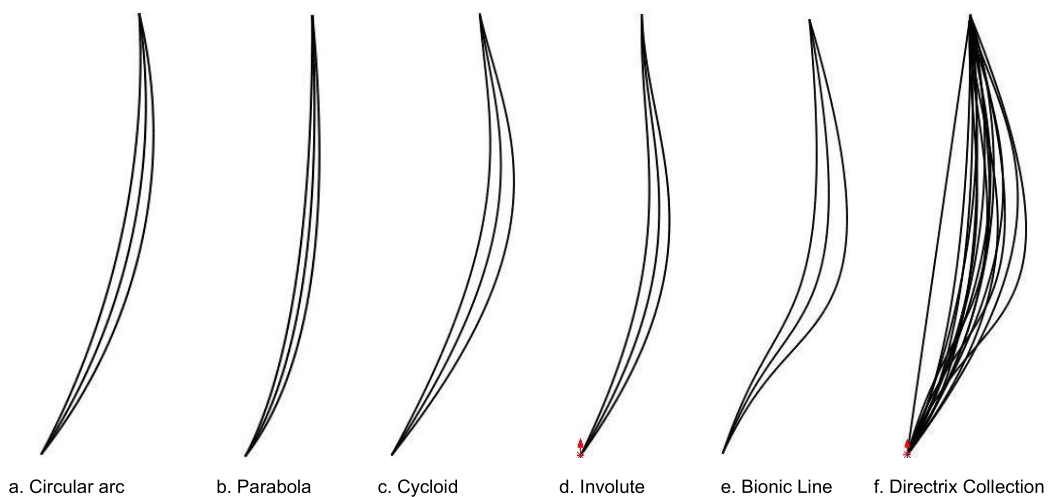
FIGURE 3. Directrix form.

2) SOIL PARAMETERS

The TE-3 soil hardness meter and ZQB-4 shear meter were used to obtain the average hardness and shear force of the test soil, combined with the "weight method" to test the soil moisture, Table 4 shows the parameters of soil characteristics.

TABLE 3. Test equipment.

No.	Name	Description
1	Bulldozing plate, Soil trough, Cart	Self-designed
2	Electric motors	PA600-type electric motor
3	Soil parameter testing instruments	ZQB-4 soil shear meter, TE-3 soil hardness meter, 110A-1 electric drying oven, balance.
4	Data acquisition and processing equipment	TJL-1 pressure sensor (3pcs)、DH-3817 Dynamic and static strain test system data acquisition box, 1394 capture card, Desktop computers Dynamic signal acquisition and analysis system.
5	Soil treatment equipment	Pickaxe, rake, shovel, sprinkler, scraper, hammer, soil suppression roller.
6	Other equipment	Tape measure, stopwatch, weight, wrench, screwdriver, vernier caliper, level, camera, wire rope.

FIGURE 4. 15 test bulldozing plates.

TABLE 4. The parameters of soil characteristics.

Soil characteristics parameters	The average hardness of soil (MPa)	Soil shear force (MPa)	Soil internal friction angle (°)	Soil cohesion (kPa)	Soil moisture content (%)
Parameter Value	0.784	20	29.83	40.9	18.15

B. SOIL TANK TEST METHOD

The specific test method is that the electric hoist pulls the cart along the track of the soil trough through the wire rope, the travel speed of the cart is 0.08m/s, and the plowing depth of the bulldozing plate is 30mm. As in Figure 6(a), the cart pushes the bulldozing plate forward through the sensor, due to the obstruction of the soil on the bulldozing plate, all three sensors will be subjected to the force, and the sensor will convert the force signal into an electrical signal and transmit it to the test system data acquisition box through the data line, the signal will be processed by the acquisition box and transmitted to the computer, and finally, the computer will present the signal in the form of data in the computer interface. The specific test principle is shown in Figure 6 (b).

The specific test contents include: (1) Installing the test equipment and testing whether the test device and software can operate normally. (2) Finishing the soil, mainly including the processes of sprinkling, tilling, raking, crushing, scraping, compaction and measuring. (3) The main soil parameters such as soil hardness, soil shear strength, soil moisture, and internal friction angle are measured according to the test requirements. (4) Measure the distance S traveled by the dolly within a period of time T with a tape measure and calculate the travel speed of the dolly according to the speed formula V=S/T. (5) Adjustment of the dozer plate and setting of software parameters. After the installation of the dozer plate is completed, the vertical and horizontal of the dozer plate is ensured by adjusting the sensor double-headed bolts. The upper sensor mainly controls the vertical direction of the dozer plate, and the left and right sensors mainly control the horizontal direction of the dozer plate. The parameter setting mainly refers to the setting of sampling frequency and channel parameters of the data acquisition box.

(a) Indoor soil trough	(b) Cart	(c) ZQB-4 type soil shear meter
(d) TE-3 type soil hardness meter	(e) PA600 type electric motor	(f) TJL-1 pressure sensor
(g) DH-3817 Dynamic and static data acquisition box	(h) 1394 capture card	(i) Data acquisition box and mainframe
(j) Glass see-through device	(k) Cart, bulldozing plate installation	(l) Sensor Installation

FIGURE 5. The test equipment.

TABLE 5. Soil adhesion evaluation criteria.

Percentage	<5%	5%-10%	10%-20%	20%-50%	>50%
Adhesion grade	minor	slight	mild	moderate	severe

The soil adhesion grade is classified as minor, slight, mild, moderate, and severe according to the degree of soil adhesion to the bulldozing plate, and the specific evaluation criterion is the percentage of soil adhesion area to the bulldozing plate area. Table 5 shows the quantified evaluation criteria for soil adhesion. Figure 7 shows a schematic diagram of each soil adhesion evaluation criterion.

C. WORKING RESISTANCE AND SOIL ADHESION ANALYSIS

Each group of tests was repeated three times, and the average of the three sets of results was taken as the final result. The test results of the working resistance and adhesion of the bulldozing plate, are shown in Table 6.

TABLE 6. Test results on working resistance and adhesion of bulldozing plate.

Directrix	Cutting angle/°	Horizontal resistance / N	Vertical resistance / N	Total resistance/N	Adherence condition
Circular arc	50	342.30	52.60	346.32	mild
Circular arc	55	321.10	48.80	324.79	mild
Circular arc	60	296.90	49.90	301.06	slight
Parabola	50	214.54	18.16	215.31	slight
Parabola	55	252.00	13.98	252.38	minor
Parabola	60	216.59	9.83	216.82	slight
Cycloid	50	289.40	44.70	292.83	minor
Cycloid	55	323.40	39.50	325.80	slight
Cycloid	60	296.20	40.30	298.93	slight
Involute	50	226.76	18.42	227.51	mild
Involute	55	238.98	5.52	239.04	minor
Involute	60	269.88	5.50	269.94	mild
Bionic Line	50	190.10	17.41	190.90	slight
Bionic Line	55	193.48	15.50	194.10	minor
Bionic Line	60	266.27	12.61	266.57	slight

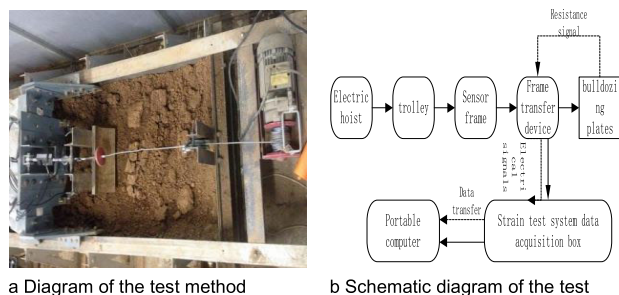a Diagram of the test method   b Schematic diagram of the test

FIGURE 6. Test method and principle.

According to Table 6, the bionic bulldozing plate has the lowest working resistance at a cutting angle of 50°. Still, the soil adhesion is not as good as that of the bionic bulldozing plate with a cutting angle of 55°. Compared to the circular bulldozing plate, the parabolic bulldozing plate reduces the horizontal working resistance by 37.32%, 21.52%, and 27.05% for cutting angles of 50°, 55°, and 60°, respectively. Cycloid bulldozing plate s decreased by 15.45%, -0.72% and 0.24%, respectively. The involute bulldozing plates decreased by 33.75%, 25.57%, and 9.10%, respectively. The bionic bulldozing plates decreased by 44.46%, 39.74%, and 10.32%, respectively.

The working resistance of the bulldozing plate mainly comes from the horizontal direction, the same directrix form of the bulldozing plate, the greater its horizontal working resistance, the more serious the soil adhesion condition. Soil fluctuation and adhesion at the front end of the bulldozing plate will be studied in the next section. The test results of the horizontal working resistance of the bulldozing plate are analyzed in Table 7.

According to Table 7, in the range of cutting angle 50° ∼ 60°, the average horizontal working resistance of the bionic bulldozing plate is the smallest, and its mechanical properties are the best, while the circular bulldozing plate is the worst. The change in cutting angle has the greatest effect on the working resistance of the bionic bulldozing plate and the least effect on the cycloidal bulldozing plate. For the five directrix forms, each bulldozing plate's average horizontal working resistance at a 50° cutting angle is the lowest, and its applicability is the best, while the 60° cutting angle is the worst. The change in directrix form has the greatest effect on the horizontal working resistance of the bulldozing plate at a 50° cutting angle and the least effect on the horizontal working resistance of the bulldozing plate at a 60° cutting angle.

V. ANALYSIS OF SOIL FLUCTUATIONS AT THE FRONT END OF THE BULLDOZING PLATE
A. SOIL FLUCTUATION TEST PROGRAM
This paper investigates the stress fluctuation behavior of the soil at the front end of the bulldozing plate under different directrix forms and cutting angle conditions. The working speed and working depth of the bulldozing plate in the test remained at 0.08m/s and 0.30m. An experimental study was conducted to investigate the dynamic behavior changes of the soil at the front end of the above 15 different directrix forms of the bulldozing plate.

The whole test needs to be repeated several times. To ensure that the state of the soil is consistent for each test, the soil needs to be pretreated before the test so that the main parameters, such as water content and hardness of the soil, are maintained within a certain range. In order to clearly capture the process of changing stress fluctuation behavior

a. minor   b. slight   c. mild   d. moderate   e. severe

FIGURE 7. Soil adhesion evaluation criteria diagram.

FIGURE 8. The soil division.

of the soil at the front end of the soil-engaging surface of the bulldozing plate, it is necessary to create multiple layers of soil and divide the entire soil tank into three areas based on the working depth of the bulldozing plate, the observed area of soil stress fluctuation behavior and the results of the commissioning test. The top area is the soil surface to the working depth of 10mm, the middle area is a 2∼5mm split area composed of white gypsum powder, and the bottom area is the lower edge of the split area to the bottom of the soil trough. The white gypsum powder was laid flat in the same position for each test, as shown in Figure 8.

B. EFFECT OF CUTTING ANGLE ON SOIL FLUCTUATIONS

When contact and interaction occur between the bulldozing plate and the soil, it produces two main effects on the soil at its front end: a cutting effect and a pushing effect. The cutting angle is an important factor influencing the change in soil fluctuation behavior. The dynamic behavior of the stresses in the soil at the front end of the bulldozing plate varies considerably for different cutting angles in the same directrix form. Analyzing 15 sets of tests, the trend of the effect of cutting angle on the change of dynamic behavior of soil stress at the front end of the bulldozing plate with different directrix forms is similar. Meanwhile, the circular directrix form is now widely used in production, and the preliminary test results show that the mechanical properties of the bionic directrix form are superior. Therefore, in this paper, the effect of the cutting angle on the change of the dynamic behavior of soil stress at the front end of the bulldozing plate is analyzed when the soil accumulation at its front end reaches a steady state,

taking the circular bulldozing plate and the bionic bulldozing plate as examples, as shown in Figure 9.

When the cutting angle is smaller, the cutting action of the bulldozing plate dominates, and the vertical force of the bulldozing plate on the soil is relatively larger at this time, which intensifies the degree of soil fluctuation and is reflected in the overturning, breaking, and fracturing of the soil, see Figure 9 (a) and (b). Specifically, the fluctuation amplitude of the soil arch at the front of the bulldozing plate (i.e., the amplitude of fluctuation on the same step fault on the white marker line) increases and this situation causes the vertical extrusion of the soil at the front end of the bulldozing plate to become larger. The vertical fluctuation of the soil increases, and adhesion is reduced. When the cutting angle increases, the soil-pushing action of the bulldozing plate dominates; at this time, the vertical force of the plate on the soil decreases, and the fluctuation of the soil at the front end of the plate decreases, which is reflected in the layering, twisting, and piling of the soil, see Figure 9 (e) and (f). This situation causes the longitudinal compression of the soil at its front end by the bulldozing plate to become larger, with increased horizontal resistance and increased adhesion.

C. EFFECT OF DIRECTRIX FORM ON SOIL FLUCTUATION

The directrix form is the main feature of the soil-engaging surface of the bulldozing plate. The variation of this feature plays the most important role in influencing the dynamic behavior of the soil at its front end. Different directrix forms of the bulldozing plate have a great influence on the soil fluctuation at its front end. Figure 10 shows the experimental diagram of the fluctuating behavior of different directrix forms of the bulldozing plate on the soil at its front end when the soil accumulation at the front end of the soil-engaging surface of the bulldozing plate reaches the basic steady state under different cutting angle conditions.

As shown in Figure 10, the fluctuating form of soil at the front end of the bulldozing plate can be classified as layering, twisting, stacking, overturning, breaking, and fracturing. Each form corresponds to a different working resistance and soil adhesion. In addition to the influence of the cutting angle, the directrix form of the soil-engaging surface of the bulldozing plate has a greater influence. The vertical resistance, soil fluctuation form, and adhesion condition of the bulldozing plate are summarized in Table 8.

TABLE 7. Result of soil resistance of plates from soil bin test.

	Cutting angle 50°	Cutting angle 55°	Cutting angle 60°	Average value	Range	Variance
Circular arc	342.30	321.10	296.90	320.10	45.40	344.03
Parabola	214.54	252.00	216.59	227.71	37.45	295.59
Cycloid	289.40	323.40	296.20	303.00	34.00	215.79
Involute	226.76	238.98	269.88	245.21	43.12	329.25
Bionic Line	190.10	193.48	266.27	216.62	76.17	1234.74

TABLE 8. Vertical resistance of the bulldozing plate, soil fluctuations, and adhesion conditions.

Directrix form	Cutting angle/°	Vertical resistance/ N	Soil fluctuation form	Bulldozing plate adhesion condition
Circular arc	50	52.60	layering, twisting, stacking,	mild
Circular arc	55	48.80	layering, twisting, stacking,	mild
Circular arc	60	49.90	overturning, breaking, and fracturing	slight
Parabola	50	18.16	layering, twisting, stacking,	slight
Parabola	55	13.98	overturning, breaking, and fracturing	minor
Parabola	60	9.83	layering, twisting, stacking,	slight
Cycloid	50	44.70	overturning, breaking, and fracturing	minor
Cycloid	55	39.50	layering, twisting, stacking,	slight
Cycloid	60	40.30	overturning, breaking, and fracturing	slight
Involute	50	18.42	layering, twisting, stacking,	mild
Involute	55	5.52	overturning, breaking, and fracturing	minor
Involute	60	5.50	layering, twisting, stacking,	mild
Bionic Line	50	17.41	overturning, breaking, and fracturing	slight
Bionic Line	55	15.50	overturning, breaking, and fracturing	minor
Bionic Line	60	12.61	layering, twisting, stacking,	mild

Combined with Figure 10 and Table 8, the fluctuation and adhesion effect of soil at the front end of the bionic and parabolic bulldozing plate is significantly better than that of the involute, circular arc, and cycloidal bulldozing plate, specifically in the form of soil overturning, breaking and fracturing caused by the bionic and parabolic bulldozing plate and less adhesion, and soil layering, twisting and stacking phenomena at the front end of the involute, circular arc and cycloidal bulldozing plate and more adhesion.

When the same directrix form, the bulldozing plate vertical resistance, the front end of the soil is more flip, broken, fracture disturbance, so soil fluctuations loose fragmentation, adhesion less. If the horizontal resistance of the bulldozing plate is large, the soil at its front end is more layered, twisted, and stacked, aggravating soil adhesion. Bionic, involute, and parabolic bulldozing plate with better soil fluctuation and adhesion even with smaller vertical resistance. And the working resistance, soil adhesion, and fluctuation of the bulldozing plate vary greatly between different directrix forms. These are all related to the curvature of the soil-engaging surface directrix and need to be analyzed comprehensively.

VI. ANALYSIS OF BULLDOZER PLATE DRAG REDUCTION AND SOIL FLUCTUATION
A. ENTROPY-BASED WEIGHTED GREY RELATIONAL RANKING
Bulldozing plate working resistance, soil adhesion, and fluctuating conditions interact with each other and are evaluated with different criteria. Bulldozing plate working resistance, soil adhesion, and fluctuating conditions interact with each other and are evaluated by different criteria. Individual performance comparisons cannot screen out the bulldozing plates with excellent overall performance, nor can they be explored in depth for their performance influence laws. Therefore, this paper proposes an entropy-weighted gray correlation analysis method to quantitatively rank the comprehensive performance of the bulldozing plates. Combining Tables 1 and 8, the horizontal resistance, vertical resistance, and total resistance of the 15 groups of bulldozing plates were selected
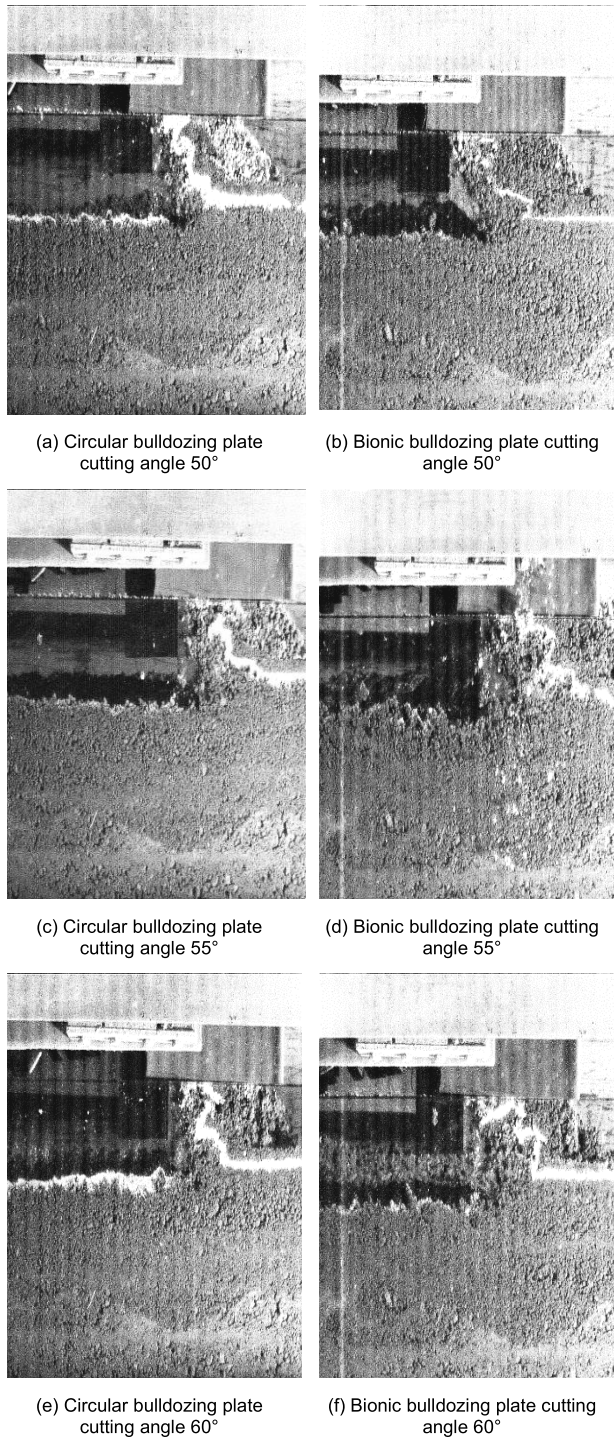
(a) Circular bulldozing plate cutting angle 50°

(b) Bionic bulldozing plate cutting angle 50°

(c) Circular bulldozing plate cutting angle 55°

(d) Bionic bulldozing plate cutting angle 55°

(e) Circular bulldozing plate cutting angle 60°

(f) Bionic bulldozing plate cutting angle 60°

FIGURE 9. The influence on soil dynamic behavior in front of bulldozing plates of cutting angle.

and ranked with soil adhesion and soil fluctuation states, respectively, as shown in Table 9 and Figure 11. The general objectives of the ranking are minimum horizontal resistance, minimum vertical resistance, minimum total resistance, minimum soil adhesion, and moderate soil fluctuation (weighting is taken as 0.5).

According to Figure 11, the total resistance, soil adhesion, and fluctuation performance of the 55° cutting angle bionic

bulldozing plate are optimal; the horizontal resistance, soil adhesion and fluctuation performance of the 55° cutting angle bionic bulldozing plate is 2nd, the horizontal resistance, soil adhesion and fluctuation performance of the 50° cutting angle bionic bulldozing plate is 3rd, the total resistance, soil adhesion and fluctuation performance of the 50° cutting angle bionic bulldozing plate is 4th, and the vertical resistance, soil adhesion and fluctuation performance of the 55° cutting angle involute bulldozing plate is 5th. The 3 sets of bionic bulldozing plate plates have the best overall performance, and the 3 sets of parabolic bulldozing plate plates also have a good and relatively stable overall performance.

B. DIRECTRIX CURVATURE AND OVERALL PERFORMANCE

Curvature is the rate of rotation of the tangential direction angle to the arc length at a point on the curve, reflecting the degree of curve deviation from a straight line, and can deeply reflect the intrinsic geometric change characteristics of the curve. Figure 12 gives the curvature variation of six typical directrix lines (straight line, circular arc, parabola, cycloid, involute, and bionic line), and explores the geometric characteristics of soil-engaging surface directrix lines in three aspects: curvature trend line, curvature radius comb, and curvature radius center trajectory, respectively, and explores the intrinsic law of its relationship with working resistance, soil adhesion and soil fluctuation.

As shown in Figure 2, the curvature trend lines of various directrix lines can be divided into three categories: constant curvature trends (straight lines and circular arcs), single-pole curvature trends (parabolic and cycloidal) and multi-pole curvature trends (bionic and involute). Where the curvature of both the bionic and parabolic front ends are convex functions, and the bipolar convex function of the bionic curvature, and contains inflection points. The normal pressure on the soil sliding over this kind of soil-engaging surface also changes, thus producing uneven fluctuations on the soil at the front end of the bulldozing plate, which is conducive to soil fragmentation and fracture, thus making the effect of soil fluctuation obvious and less adhesion. From the slip line field theory [23], this geometric feature is advantageous for the rapid formation of slip fracture surfaces, reducing the internal frictional resistance of the soil, etc. Although it will increase the vertical force, the increase in vertical force is small and a small percentage of the total resistance, and this fluctuation reduces the soil adhesion of the bulldozing plate and significantly reduces the horizontal resistance, thus reducing the overall working resistance.

Therefore, a hypothesis is proposed: (1) The directrix curvature of the soil-engaging surface contains convex functions, multi-extremum points, inflection points, or bulldozing plates with non-differentiable points, which can significantly enhance the fluctuation of the soil at the front end of the bulldozing plate, reduce soil adhesion, and reduce the horizontal working resistance and total working resistance of the bulldozing plate. (2) For the bulldozing plate with the same directrix form of soil-engaging surface, the different cutting
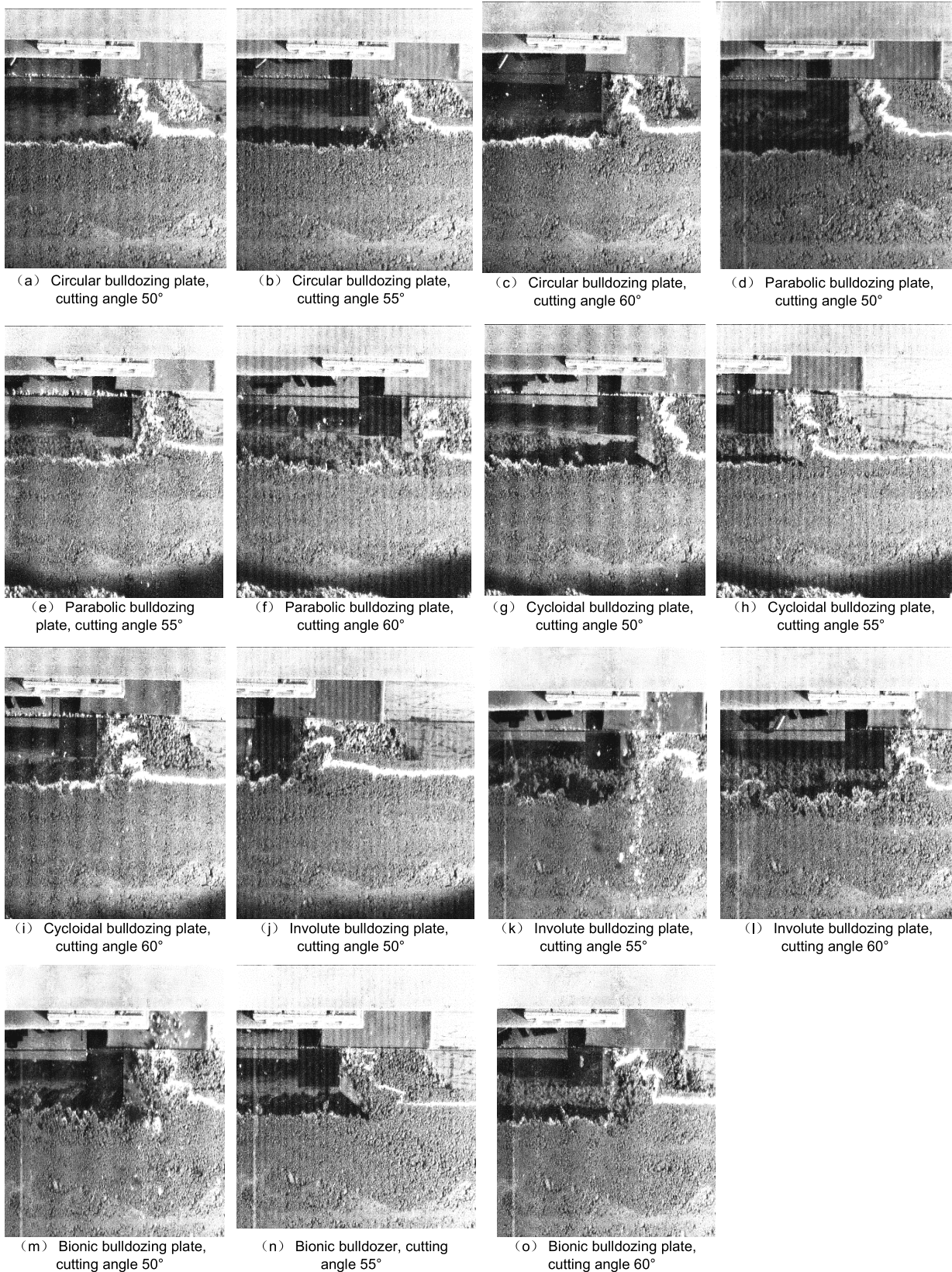
（a）Circular bulldozing plate, cutting angle 50°

（b）Circular bulldozing plate, cutting angle 55°

（c）Circular bulldozing plate, cutting angle 60°

（d）Parabolic bulldozing plate, cutting angle 50°

（e）Parabolic bulldozing plate, cutting angle 55°

（f）Parabolic bulldozing plate, cutting angle 60°

（g）Cycloidal bulldozing plate, cutting angle 50°

（h）Cycloidal bulldozing plate, cutting angle 55°

（i）Cycloidal bulldozing plate, cutting angle 60°

（j）Involute bulldozing plate, cutting angle 50°

（k）Involute bulldozing plate, cutting angle 55°

（l）Involute bulldozing plate, cutting angle 60°

（m）Bionic bulldozing plate, cutting angle 50°

（n）Bionic bulldozer, cutting angle 55°

（o）Bionic bulldozing plate, cutting angle 60°

FIGURE 10. Soil fluctuation behavior at the front end of the bulldozing plate with different directrix forms.

TABLE 9. Comprehensive performance quantitative ranking tables.

Conductor number	1	2	3	4	5
Horizontal resistance	0.537756	0.548387	0.665450	0.791482	0.7275489
Vertical resistance	0.528508	0.535216	0.629568	0.754579	0.783978
Total resistance	0.545956	0.558159	0.677009	0.83395	0.751757
Second group	6	7	8	9	10
Horizontal resistance	0.786777	0.67099	0.80194	0.648965	0.789704
Vertical resistance	0.802861	0.639425	0.7955	0.633404	0.775345
Total resistance	0.829278	0.684018	0.812291	0.661775	0.823953
Third group	11	12	13	14	15
Horizontal resistance	0.74543	0.687915	0.890796	0.906318	0.691518
Vertical resistance	0.874402	0.855894	0.781731	0.821922	0.776519
Total resistance	0.775079	0.70748	0.878699	0.919548	0.711899

a. Horizontal resistance, adhesion, and fluctuation sorting

b. Vertical resistance, adhesion, and fluctuation sorting

c. Total resistance, adhesion, and fluctuation sorting

d. Aggregate Comparison
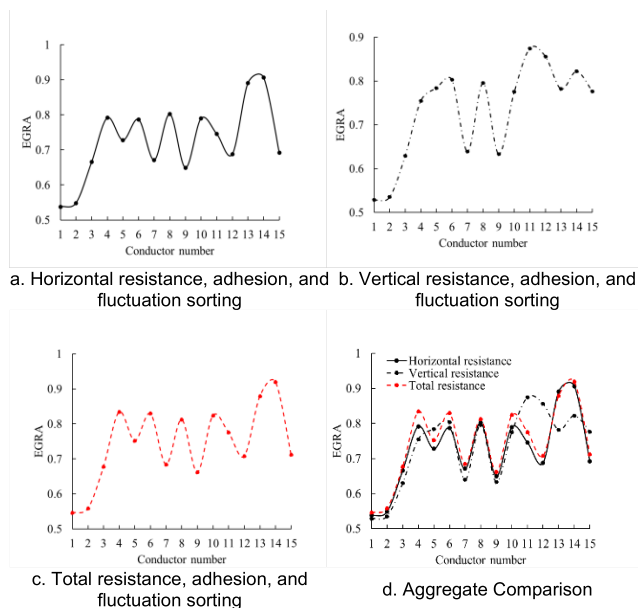
FIGURE 11. Resistance, adhesion, and fluctuation entropy weighted gray relational ranking.

a. *Straight line*

b. *Circular arc*

c. *parabolic*

d. *cycloid*

e. *involute*

f. *bionic line*

FIGURE 12. The change trends of five line curvature.

angles, namely the different inclination angles of the soil-engaging surface directrix, differ from the directrix equation of the soil coordinate system. Although the relative curvature, convexity and concavity, poles, and inflection points of the directrix remain unchanged, their absolute values change in the working coordinate system of the bulldozing plate and the soil. Therefore, the change of cutting angle is essentially still the change of the curvature of the soil-engaging surface directrix relative to the soil. Although this change has no great influence on the change of directrix form, it determines the magnitude of vertical working resistance and the fluctuation of soil. (3) Under the same directrix form of soil-engaging surface, the large vertical resistance makes the soil flip, break, break, and other fluctuations obviously, reduces the soil adhesion, and significantly reduces the horizontal working resistance, thereby reducing the total working resistance; the small vertical resistance reduces the soil fluctuation effect, makes the soil strat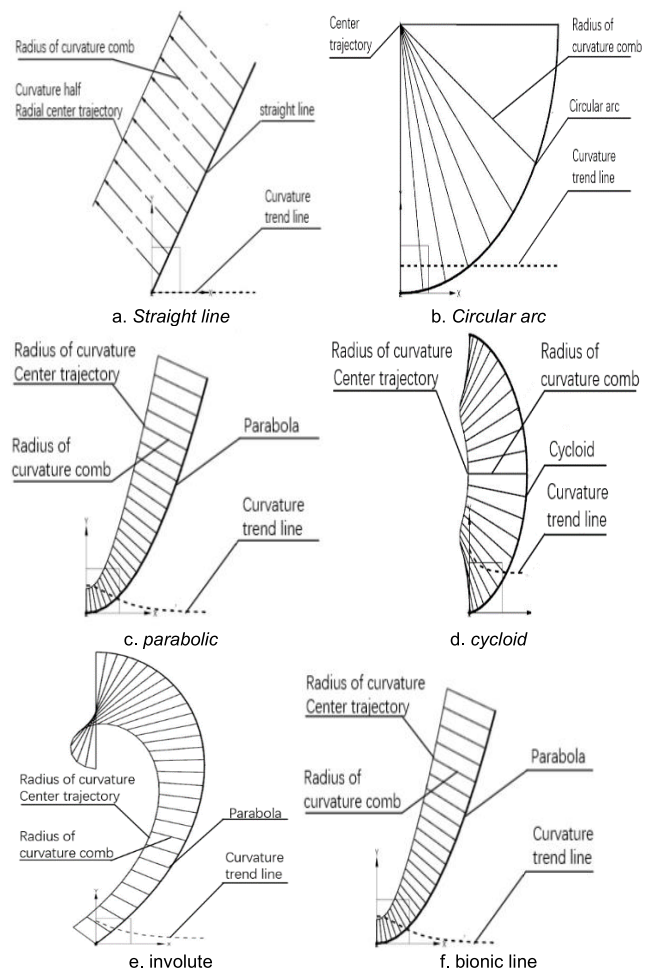ification, distortion, and accumulation obvious, reduces the soil adhesion, significantly increases the horizontal working resistance, and increases the total working resistance.

VII. CONCLUSION

In this paper, 15 groups of bulldozing plates with arc type, parabolic type, cycloid type, involute type, and bionic type are

designed. The soil-bin test studies the reducing adhesion and resistance performance of each bulldozing plate. The influence law of the comprehensive mechanical properties of bulldozing plate soil engaging surface was analyzed regarding macroscopic mechanical properties and microscopic intrinsic curvature.

1. Combined with the entropy-weighted gray correlation analysis method, a comprehensive evaluation and quantitative ranking method for the performance of the working resistance, soil adhesion, and soil fluctuation of the bulldozing plate is proposed, which provides a methodological guide for the investigation of the intrinsic influencing factors of the excellent performance of the bulldozing plate. The test shows that the bionic bulldozing plate has good resistance and adhesion reduction performance and can be optimized by optimizing the collinear form and cutting angle to achieve the optimal design of soil touching the surface of construction machinery such as bulldozing plate.

2. A hypothesis is proposed: (1) The directrix curvature of the soil engaging surface contains convex functions, multi-extremum points, inflection points, or bulldozing plates with non-differentiable points, which can significantly enhance the fluctuation of the soil at the front end of the bulldozing plate, reduce soil adhesion, and reduce the horizontal working resistance and total working resistance of the bulldozing plate. (2) For the bulldozing plate with the same directrix form of soil engaging surface, the different cutting angles, namely the different inclination angles of the soil engaging surface directrix, differ from the directrix equation of the soil coordinate system. Although the relative curvature, convexity and concavity, poles, and inflection points of the directrix remain unchanged, their absolute values change in the working coordinate system of the bulldozing plate and the soil. Therefore, the change of cutting angle is essentially still the change of the curvature of the soil engaging surface directrix relative to the soil. Although this change has no great influence on the change of directrix form, it determines the magnitude of vertical working resistance and the fluctuation of soil. (3) Under the same directrix form of soil engaging surface, the large vertical resistance makes the soil flip, break, break and other fluctuations obviously, reduces the soil adhesion, and significantly reduces the horizontal working resistance, thereby reducing the total working resistance; the small vertical resistance reduces the soil fluctuation effect, makes the soil stratification, distortion, and accumulation obvious, reduces the soil adhesion, significantly increases the horizontal working resistance, and increases the total working resistance.

3. Prospects for later research: Through experiments, the soil engaging surface of the bulldozing plate with excellent performance is selected, and the variation law of its directrix curvature is analyzed. A new curvature function that conforms to the hypothesis of this paper is spliced or optimized by using a similar gene editing method. Then, the directrix equation is obtained by the method of curvature reverse, and then a new soil engaging surface is constructed to realize the optimal performance design of the bulldozing plate.

REFERENCES

[1] H. Yu, Z. Han, J. Zhang, and S. Zhang, "Bionic design of tools in cutting: Reducing adhesion, abrasion or friction," *Wear*, vols. 482–483, Oct. 2021, Art. no. 203955.

[2] J. Yu, Y. Ma, S. Wang, Z. Xu, X. Liu, H. Wang, H. Qi, L. Han, and J. Zhuang, "3D finite element simulation and experimental validation of a mole rat's digit inspired biomimetic potato digging shovel," *Appl. Sci.*, vol. 12, no. 3, p. 1761, Feb. 2022.

[3] Y. Yang, J. Tong, Y. Huang, J. Li, and X. Jiang, "Biomimetic rotary tillage blade design for reduced torque and energy requirement," *Appl. Bionics Biomech.*, vol. 2021, Sep. 2021, Art. no. 8573897.

[4] Z. Chongren, "Russia's new model of construction machinery," *Construct. Machinery Equip.*, vol. 41, no. 7, pp. 55–56, 2010.

[5] B. Szabo, F. Barnes, S. Sture, and H.-Y. Ko, "Effectiveness of vibrating bulldozer and plow blades on draft force reduction," *Trans. ASAE*, vol. 41, no. 2, pp. 283–290, 1998.

[6] K. Araya, "Soil failure caused by subsoilers with pressurized water injection," *J. Agricult. Eng. Res.*, vol. 58, no. 4, pp. 279–287, Aug. 1994.

[7] K. Sakai, S. I. Hata, M. Takai, and S. Nambu, "Design parameters of four-shank vibrating subsoiler," *Trans. ASAE*, vol. 36, no. 1, pp. 23–26, 1993.

[8] T. Zhicheng, "Analysis of energy-saving and emission-reduction in construction and machinery industry," *Construct. Machinery Technol. Manage.*, vol. 23, no. 10, pp. 55–56, 2010.

[9] Z. Chongren, "New approach of energy saving and consumption reduction to construction machine," *Construct. Machinery Equip.*, vol. 7, pp. 65–66, Aug. 2010.

[10] G. Yun-Qing, M. Jie-Gang, D. Dong-Shun, Z. Shui-Hua, J. Lan-Fang, W. Deng-Hao, R. Yun, and L. Fu-Qing, "Characteristics on drag reduction of bionic jet surface based on earthworm's back orifice jet," *Acta Phys. Sinica*, vol. 64, no. 2, 2015, Art. no. 024701.

[11] X. Li, S. Wang, H. Meng, Q. Qu, and Y. Jia, "Research on drag reduction mechanism of pneumatic subsoiler and establishment of resistance mathematical model," *Can. J. Soil Sci.*, vol. 102, no. 2, pp. 531–548, Jun. 2022.

[12] S. Zuo, D. Kong, L. Liu, X. Dong, and Y. Zhao, "Experiment on the effect of air-pressure subsoiling based on air-pressure cracking theory," *Trans. Chin. Soc. Agricult. Eng.*, vol. 32, no. 1, pp. 54–61, 2016.

[13] H. Zhang, K. Araya, M. Kudoh, C. Zhang, H. Jia, F. Liu, T. Sawai, and S. Yang, "An explosive subsoiler for the improvement of meadow soil—Part 1: Thermodynamics," *J. Agricult. Eng. Res.*, vol. 75, no. 1, pp. 97–105, Jan. 2000.

[14] I. Keppler, Z. Hudoba, I. Oldal, A. Csatar, and L. Fenyvesi, "Discrete element modeling of vibrating tillage tools," *Eng. Comput.*, vol. 32, no. 2, pp. 308–328, Apr. 2015.

[15] G. Liu, J. Xia, K. Zheng, J. Cheng, K. Wang, R. Zeng, H. Wang, and Z. Liu, "Effects of vibration parameters on the interfacial adhesion system between soil and metal surface," *Soil Tillage Res.*, vol. 218, Apr. 2022, Art. no. 105294.

[16] T. Niyamapa and V. M. Salokhe, "Force and pressure distribution under vibratory tillage tool," *J. Terramech.*, vol. 37, no. 3, pp. 139–150, Jul. 2000.

[17] L. Ren, Q. Cong, J. Tong, and B. Chen, "Reducing adhesion of soil against loading shovel using bionic electro-osmosis method," *J. Terramech.*, vol. 38, no. 4, pp. 211–219, Oct. 2001.

[18] J. Massah, M. R. Fard, and H. Aghel, "An optimized bionic electro-osmotic soil-engaging implement for soil adhesion reduction," *J. Terramech.*, vol. 95, pp. 1–6, Jun. 2021.

[19] L. Ren, Z. Han, J. Li, and J. Tong, "Effects of non-smooth characteristics on bionic bulldozer blades in resistance reduction against soil," *J. Terramech.*, vol. 39, no. 4, pp. 221–230, Oct. 2002.

[20] L.-Q. Ren, J. Tong, J.-Q. Li, and B.-C. Chen, "Soil adhesion and biomimetics of soil engaging components: A review," *J. Agricult. Eng. Res.*, vol. 79, no. 3, pp. 239–264, 2001.

[21] B. Chirende, J. Li, L. Wen, and T. E. Simalenga, "Effects of bionic non-smooth surface on reducing soil resistance to disc ploughing," *Sci. China Technol. Sci.*, vol. 53, no. 11, pp. 2960–2965, Nov. 2010.

[22] B. Wu, R. Zhang, P. Hou, J. Tong, D. Zhou, H. Yu, Q. Zhang, J. Zhang, and Y. Xin, "Bionic nonsmooth drag reduction mathematical model construction and subsoiling verification," *Appl. Bionics Biomech.*, vol. 2021, Nov. 2021, Art. no. 5113453.

[23] J. Niu, T. Luo, J. Xie, H. Cai, Z. Zhou, J. Chen, and S. Zhang, "Simulation and experimental study on drag reduction and anti-adhesion of subsoiler with bionic surface," *Int. J. Agricult. Biol. Eng.*, vol. 15, no. 4, pp. 57–64, 2022.

[24] H. Zhao, H. Li, S. Ma, J. He, Q. Wang, C. Lu, Z. Zheng, and C. Zhang, "The effect of various edge-curve types of plain-straight blades for strip tillage seeding on torque and soil disturbance using DEM," *Soil Tillage Res.*, vol. 202, Aug. 2020, Art. no. 104674.

[25] Y. He, P. Lu, L. Guo, and W. Wu, "Effect of horizontal plate length on working resistance of blade under different cutting rake angles," in *Proc. 5th Int. Conf. ElectroMechanical Control Technol. Transp. (ICECTT)*, May 2020, pp. 141–144.

[26] B. Li, Y. Chen, and J. Chen, "Modeling of soil–claw interaction using the discrete element method (DEM)," *Soil Tillage Res.*, vol. 158, pp. 177–185, May 2016.

[27] Y. He, J. Zhang, L. Guo, C. Zhang, and P. Lu, "Effect of horizontal plate length on cutting resistance of blade under different cutting depths in a sandy soil," *Arabian J. Sci. Eng.*, vol. 46, no. 12, pp. 11661–11669, Dec. 2021.

[28] S. H. Hoseinian, A. Hemmat, A. Esehaghbeygi, G. Shahgoli, and A. Baghbanan, "Development of a dual sideway-share subsurface tillage implement—Part 2. Effect of tool geometry on tillage forces and soil disturbance characteristics," *Soil Tillage Res.*, vol. 215, Jan. 2022, Art. no. 105200.

[29] K. A. Aikins, J. B. Barr, M. Ucgul, T. A. Jensen, D. L. Antille, and J. M. A. Desbiolles, "No-tillage furrow opener performance: A review of tool geometry, settings and interactions with soil and crop residue," *Soil Res.*, vol. 58, no. 7, pp. 603–621, 2020.

[30] W. R. Gill and G. E. Vanden Berg, Eds., *Soil Dynamics in Tillage and Traction* (Agricultural Handbook no. 316). Washington, DC, USA: Superintendent of Documents, U.S. Government Printing Office, May 1968, p. 512, doi: 10.2136/sssaj1968.03615995003200030005x.

[31] Z. Guo, Z. Zhou, Y. Zhang, and Z. Li, "Bionic optimization research of soil cultivating component design," *Sci. China E, Technol. Sci.*, vol. 52, no. 4, pp. 955–965, Apr. 2009.

[32] R. J. Godwin, "A review of the effect of implement geometry on soil failure and implement forces," *Soil Tillage Res.*, vol. 97, no. 2, pp. 331–340, Dec. 2007.

[33] J. Mak, Y. Chen, and M. A. Sadek, "Determining parameters of a discrete element model for soil–tool interaction," *Soil Tillage Res.*, vol. 118, pp. 117–122, Jan. 2012.

[34] Z.-J. Guo and L.-W. Ni, "The analysis of soil engaging surface of bulldozing plate based on the adjacent structure of elliptic point," in *Proc. Int. Conf. Design, Manuf. Mechatronics (ICDMM)*, Wuhan, China, 2016, pp. 940–945.

[35] S. Zhang and Z.-J. Guo, "Study on the geometrical properties and working resistance performance of bionic bulldozing plate," in *Proc. Int. Conf. Adv. Mech. Syst. (ICAMechS)*, Luoyang, China, Sep. 2013, pp. 280–285.

[36] Q. H. Wu, *Engineering Machinery Design*. Wuhan, HB, China: Wuhan Univ. Press, 2006.

ZHIJUN GUO (Member, IEEE) received the bachelor's degree in vehicle engineering from the Henan University of Science and Technology, Luoyang, China, in 1992, the master's degree in vehicle design and manufacturing from the Jilin University of Technology, in 1995, and the Ph.D. degree in agricultural mechanization engineering from Lin University, in 2002. He has been teaching with the School of Vehicle and Traffic Engineering, Henan University of Science and Technology, since 1995. His research interests include vehicle, mechanical system dynamics, soil cutting dynamics, and intelligent vehicle control.

SHUAI ZHANG (Member, IEEE) received the B.S. and M.S. degrees in vehicle engineering from the Henan University of Science and Technology, Luoyang, China, in 2011 and 2014, respectively, and the Ph.D. degree in vehicle engineering from Jilin University, Jilin, China, in 2018. Since 2018, he has been a Lecturer with the College of Vehicle and Traffic Engineering, Henan University of Science and Technology. His research interests include research and innovation of automobile structure design theory and key technology.

LIWEI NI received the M.S. degree from the Henan University of Science and Technology, in 2015, and the Ph.D. degree in vehicle engineering from Jilin University, Jilin, China, in 2021. He is currently a Lecturer with the College of Mechanical Engineering, Henan University of Engineering, China. His research interests include wheel-legged robot and all-terrain vehicle.

• • •